TiS Trends in Sciences
TRENDS IN SCIENCES 2027; 24(1): 14114
SPRINT Scholarly Publishing and Repository Integration Center
https://doi.org/10.48048/tis.2027.14114
RESEARCH ARTICLE

Glinus oppositifolius (L.) Aug. DC. Ethanolic Extract Attenuates Hydrogen Peroxide-Induced Oxidative Stress and Modulates Apoptosis-Related Gene Expression in HepG2 Cells via Activation of the Nrf2-ARE Signaling Pathway

Alisa Naladta[1], Natsajee Nualkaew[2], Liudmila Yarovaya[3], Santi Phosri[4], La-or Somsakeesit[5], Khomsorn Lomthaisong[1] and Anupong Joompang[3,*]

[1]*Department of Biochemistry, Faculty of Sciences, Khon Kaen University, Khon Kaen 40002, Thailand*
[2]*Division of Pharmacognosy and Toxicology, Faculty of Pharmaceutical Sciences, Khon Kaen University, Khon Kaen 40002, Thailand*
[3]*Faculty of Pharmaceutical Sciences, Burapha University, Chonburi 20131, Thailand*
[4]*Department of Chemical Engineering, Faculty of Engineering, Burapha University, Chonburi 20131, Thailand*
[5]*Department of Chemistry, Faculty of Engineering, Rajamangala University of Technology Isan Khon Kaen Campus, Khon Kaen 40000, Thailand*

([*]Corresponding author's e-mail: anupong.jo@go.buu.ac.th)

Received: 17 April 2026, Revised: 16 May 2026, Accepted: 8 June 2026, Published: 10 August 2026

Abstract

Oxidative stress plays a pivotal role in the development of liver damage, and natural antioxidants have emerged as promising candidates for its prevention. Therefore, this study investigated the protective effects and mechanisms of the Thai local *Glinus oppositifolius* (Linn.) Aug. DC. ethanolic extract (GOE) against hydrogen peroxide (H_2O_2)-induced oxidative stress in HepG2 cells. GOE pretreatment at 3.125 - 25 µg/mL protected the cells against H_2O_2-induced oxidative stress without causing cytotoxicity and significantly reduced intracellular reactive oxygen species (ROS) levels. The extract also showed anti-inflammatory activity by decreasing nitric oxide (NO) production in lipopolysaccharide (LPS)-induced RAW 264.7 cells. Metabolomic profiling analysis revealed that GOE contained a wide range of bioactive metabolites, with phenylpropanoids, flavonoids, terpenoids, and saponins as the major groups likely contributing to its biological activity. Network pharmacology analysis suggested that the protective effect of GOE was associated with the regulation of apoptosis and the Nrf2-ARE signaling pathway. Albiflorin, oleanolic acid, vitexin, isovitexin, acetyl-vitexin, and agnuside are candidate contributors to the protective effect of GOE. Real-time PCR further indicated that GOE modulated apoptosis by downregulating TNF-α, p53, Bax, and Casp3, while upregulating Bcl-2 gene expression. In addition, GOE modulated the Nrf2-ARE signaling pathway by reducing Keap1 and increasing Nrf2, SOD, CAT, HO-1, and NQO1 gene expression. Overall, GOE appears to be a promising source of bioactive phytochemicals for protection against ROS-induced hepatic oxidative stress and may have potential for further pharmaceutical and nutraceutical investigation.

Keywords: *Glinus oppositifolius*, Hepatoprotection, Oxidative stress, Nrf2-ARE pathway, Apoptosis, HepG2 cells, Antioxidant enzymes

Introduction

Oxidative stress results from an imbalance between reactive oxygen species (ROS) and the antioxidant defense system. Excessive ROS can react with proteins, lipids, and DNA, leading to oxidative stress-related diseases, including liver dysfunction, diabetes, obesity, cancer, and neurological disorders [1]. The liver is particularly vulnerable to oxidative stress, as it is the major site of metabolic and detoxification activities, both of which are closely linked to ROS

production [2,3]. Among the ROS involved, $O_2^{\bullet-}$ and H_2O_2 are important contributors to hepatic damage and dysfunction, which may further promote liver pathogenesis [4].

Liver injury is also closely associated with lipopolysaccharide (LPS). Elevated levels of LPS can trigger damage of hepatocytes and activate hepatic macrophages, leading to the production of pro-inflammatory cytokines, including tumor necrosis factor (TNF)-α, interleukin (IL)-1β, and IL-6, together with additional ROS production. This process promotes liver inflammation, oxidative damage [5,6], and, ultimately, cell apoptosis, all of which contribute to the progression of liver diseases [2]. In this context, the Nrf2-ARE pathway is a major cellular defense mechanism against oxidative stress and inflammation in liver cells, regulating the cellular antioxidant response and preventing excessive ROS [7]. An impairment of this pathway has been linked to chronic liver disorders [8].

Emerging evidence indicates the potential of various plant-derived compounds to mitigate oxidative liver damage by modulating the Nrf2-ARE signaling pathway. This activation increases the expression of antioxidant enzymes that remove excess ROS and strengthen the cellular antioxidant defense system [9]. Therefore, plant phytochemicals may serve as useful natural agents for preventing hepatic oxidative stress and inflammation.

Glinus oppositifolius has attracted growing interest due to its wide range of pharmacological activities. Its methanolic extract has been reported to exhibit antioxidant [10] and anti-inflammatory activities [11]. In addition, the extract reduced oxidative stress and inflammatory biomarkers in Complete Freund's Adjuvant (CFA)-induced arthritis [12]. A diverse range of bioactive constituents has been identified in this plant, including aromatic compounds, steroids, flavonoid glycosides, triterpenoid saponins, and polysaccharides [13]. Moreover, spergulagenin B, C, and D have shown anti-inflammatory activity in LPS-induced RAW 264.7 cells [14]. These findings suggest that *G. oppositifolius* may help mitigate oxidative stress and provide therapeutic benefits against oxidative stress and inflammation, making it a promising candidate for natural drug development. However, despite its well-established antioxidant and anti-inflammatory properties, there are still no studies, to the best of our knowledge, investigating the effects of *G. oppositifolius* on H_2O_2-induced oxidative stress in HepG2 cells.

Therefore, this study aimed to evaluate the protective effect of *G. oppositifolius* extract against H_2O_2-induced oxidative stress in HepG2 cells and anti-inflammatory activity in RAW 264.7 cells. Moreover, the phytochemical profiling of *G. oppositifolius* collected in Thailand was investigated using metabolomic analysis to facilitate the identification of bioactive compounds relevant to the development of standardized extraction protocols. This research is expected not only to bridge the existing knowledge gap but also to provide scientific evidence for the future use of *G. oppositifolius* as a natural agent against oxidative stress in liver cells for pharmaceutical and nutraceutical investigation.

Materials and methods

Chemicals and reagents

Dimethyl sulfoxide (DMSO) and ethanol were purchased from RCI Labscan Co. Ltd., Ireland. Crystal violet was obtained from QRëC, New Zealand. Hydrogen peroxide (H_2O_2) was purchased from Fisher Scientific, UK. 3-(4,5-Dimethylthiazol-2-yl)-2,5-diphenyltetrazolium bromide (MTT), lipopolysaccharide (LPS), 2′,7′-dichlorofluorescein diacetate (DCFH-DA), and L-nitro-arginine methyl ester (L-NAME) were obtained from Sigma-Aldrich, USA. TRIzol reagent was purchased from Molecular Research Center, Inc., USA. RevertAid First Strand cDNA Synthesis Kit and Maxima SYBR Green qPCR Master Mix were obtained from Thermo Fisher Scientific, USA.

Methods

Plant collection and identification

The whole plants of *G. oppositifolius* (L.) Aug. DC. were collected from Khon Kaen Province, Thailand (**Figure 1**). Botanical identification was performed by Associate Professor Suppachai Tiyaworanant. A voucher specimen (No. 3672-KKPSH010102980) was deposited at the Herbarium of the Faculty of Pharmaceutical Sciences, Khon Kaen University, Thailand.



Figure 1 Morphological features of *G. oppositifolius* (L.) Aug. DC. (A) whole plants and (B) flower, leaf, and stem parts.

Preparation of G. oppositifolius extracts

The plant material was cleaned, dried in a hot air oven at 40 °C for 48 h, and pulverized. The powdered material was then macerated in 80% ethanol at a ratio of 1:10 (w/v) for 2 cycles, each lasting 3 - 4 days. The filtrates were concentrated under reduced pressure using a rotary evaporator and then freeze-dried to obtain the dried *G. oppositifolius* extract (GOE). The extract was stored in an airtight container at –20 °C until use.

Cell culture

Vero (ATCC CCL-81), HepG2 (ATCC HB-8065), and RAW 264.7 cells (ATCC TIB-71) were cultivated in Dulbecco's Modified Eagle Medium (DMEM; Hyclone-Cytiva, USA) supplemented with 10% fetal bovine serum (FBS; Sigma- Aldrich, France) and 1% Antibiotic-Antimycotic (Hyclone-Cytiva, USA) at 37 °C and 5% CO_2.

Cell viability assay

The cytotoxicity of GOE toward Vero, HepG2, and RAW 264.7 cells was evaluated using the MTT assay. Vero cells (1.0×10^4 cells/well), HepG2 cells (2.5×10^4 cells/well), and RAW 264.7 cells (2.5×10^4 cells/well) were seeded into 96-well plates and incubated overnight. The cells were then treated with GOE at different concentrations of 0 - 600, 0 - 500, and 0 - 200 µg/mL for Vero, HepG2, and RAW 264.7 cells, respectively. DMSO (0.2% (v/v)) was used as the control. After 24, 48, and 72 h of treatment, the supernatant was discarded, and the cells were rinsed with 1 × PBS. MTT solution (0.5 mg/mL) was then added, and the plates were incubated for 3 h. The formazan crystals were solubilized in DMSO, and absorbance was measured at 570 nm using an EnSight Multimode Plate Reader (Perkin Elmer, USA). Cell viability was expressed as a percentage relative to the untreated control group.

Protective effect assay

HepG2 cells (2.5×10^4 cells/well) were seeded in 96-well plates and incubated for 24 h. The cells were then pretreated with various concentrations of GOE (0 - 50 µg/mL) in a low-serum medium containing 2% FBS for 24 h. DMSO (0.2% v/v) was used as the control. Oxidative stress was subsequently induced by treatment with 1 mM H_2O_2 in 2% FBS medium for a further 24 h. After treatment, 50 µL of MTT solution (0.5 mg/mL in 1×PBS) was added to each well, and the plates were incubated at 37 °C for 2 h. The resulting formazan crystals were dissolved in 100 µL of DMSO, and the absorbance was measured at 570 nm using a microplate reader. The results were expressed as the percentage of cell viability relative to the control group.

NO production assay

RAW 264.7 cells (2.0×10^4 cells/well) were seeded into 96-well plates for 24 h. The cells were then co-treated with LPS (250 ng/mL) and GOE (0 - 200 µg/mL). DMSO (0.2%) and L-NAME (200 µM) were used as negative and positive controls, respectively. After 24 h of treatment, 50 µL of the culture medium was mixed with 50 µL of Griess reagent, and the absorbance was measured at 540 nm. The results were expressed as the percentage of NO production relative to the LPS-treated group. Cell viability was then determined using the MTT assay, as described in the Cell viability assay, and expressed as a percentage relative to the untreated control group.

Intracellular ROS assay

HepG2 cells (2.0×10^5 cells/well) were seeded into 24-well plates and incubated for 24 h. The cells were then pretreated with GOE (0 - 50 µg/mL) in low-serum medium containing 2% FBS for 24 h. DMSO (0.2% (v/v)) was used as the control. After pretreatment, intracellular ROS production was induced by incubation with 1.0 mM H_2O_2 in 2% FBS medium for 4 h. The medium was then removed, and cells were washed once with 1×PBS before incubation with 20 µM DCFH-DA at 37 °C for 30 min in the dark. After incubation, the cells were washed 3 times with 1xPBS, and the fluorescence intensity was measured at 485/535 nm. Representative images of intracellular ROS levels were then captured immediately using an EVOS™ Auto 2 (Invitrogen; Thermo Fisher Scientific, USA). The images were acquired using a 20× objective lens and a GFP light cube (excitation/emission: 470/510 nm) to visualize the green fluorescence of DCF. To account for variations in cell number, the fluorescence intensity of DCFH-DA was normalized to the total biomass using the crystal violet staining method, as previously described [15]. The results were expressed as relative fluorescence units (RFU) and compared with the H_2O_2-treated group using the following formula:

$$ROS\ (\%\ of\ control) = (F_{sample} - F_{blank})/(F_{control} - F_{blank})\times100$$

where F represents the fluorescence value [16].

Reverse transcription quantitative real-time polymerase chain reaction (RT-qPCR) analysis

HepG2 cells (2.5×10^5 cells/well) were seeded in 6-well plates and incubated for 24 h. The cells were then pretreated with GOE extract (0.625 - 25 µg/mL) using DMSO (0.2% (v/v)) as the control and subsequently exposed to H_2O_2 using a protocol similar to that described in the Protective effect assay. After 24 h of H_2O_2 treatment, total RNA was extracted from the HepG2 cells using TRIzol reagent (Molecular Research Center, Inc., USA) according to the manufacturer's instructions. Subsequently, 3 µg of total RNA was reverse-transcribed using the RevertAid First Strand cDNA Synthesis Kit (Thermo Fisher Scientific, Lithuania). Quantitative real-time PCR was conducted using the CFX96 Real-Time PCR Detection System (Bio-Rad, Singapore) and 2× Maxima SYBR Green qPCR Master Mix (Thermo Fisher Scientific, Lithuania). The target genes related to inflammatory responses and antioxidant enzymes are specified in **Table 1**. Primer sequences were designed using the NCBI Primer-BLAST tool and synthesized by Bionics (Korea). The GAPDH gene served as the internal housekeeping control for normalization. Relative mRNA expression levels were calculated using the $2^{-\Delta\Delta Ct}$ method [17].

Table 1 PCR primers.

Gene	Primer Sequences (5' → 3')	Size (bp)	Accession Number
Keap1	GCATCCACCACAACAGTGTG AGGAGACGATTGAGGACAGC	115	NM_203500.2
Nrf2	GACATTGAGCAAGTTTGGGAGG CAGTTTGGCTTCTGGACTTGGA	114	NM_006164.5
SOD1	CTCACTCTCAGGAGACCATTGC CAAGCCAAACGACTTCCAGC	126	NM_000454.5
CAT	AGCCTACGTCCTGAGTCTCT TGATGCCCTGGTCAGTCTTA	169	NM_001752.4
HO-1	TTCAAGCAGCTCTACCGCTC TTGGTGTCATGGGTCAGCAG	146	NM_002133.3
NQO1	TCGGCAGAAGAGCACTGATC GAAGTTCATGGCATAGAGGTCCG	137	NM_000903.3
TNFα	GACAAGCCTGTAGCCCATGTT CTGGTTATCTCTCAGCTCCACG	114	NM_000594.4
P53	TGTGACTTGCACGTACTCCC ACCATCGCTATCTGAGCAGC	199	NM_000546.6

Gene	Primer Sequences (5' → 3')	Size (bp)	Accession Number
Bax	CTGACGGCAACTTCAACTGG CATGATGGTTCTGATCAGTTCCG	110	NM_138761.4
Bcl-2	CCCTCGTCCAAGAATGCAA CCATCCTTCCCAGAGGAAAAG	136	NM_000633.3
Casp3	GAAGCGAATCAATGGACTCTGG ATCGACATCTGTACCAGACCGA	143	NM_004346.4
GAPDH	GAAAGCCTGCCGGTGACTAA AGGAAAAGCATCACCCGGAG	120	NM_001256799.3

LC-QTOF-MS analysis

LC-QTOF-MS-based metabolite profiling was performed to obtain an exploratory qualitative chemical fingerprint for putative metabolite characterization. The GOE (10.4 mg) was extracted with 1 mL of 70% methanol containing 50 ng/mL sulfadimethoxine as an internal standard. The extract was sonicated for 35 min and then centrifuged at 14,000 rpm for 10 min. The supernatant was collected and diluted 2-fold with 70% methanol containing 50 ng/mL sulfadimethoxine, followed by LC-MS analysis. Metabolites were tentatively annotated using an Agilent 1290 Infinity II Bio LC system coupled with an Agilent 6545XT Quadrupole Time-of-Flight (QTOF) mass spectrometer (Agilent Technologies, USA). Chromatographic separation was performed on a Poroshell 120 EC-C18 column (2.1×100 mm, 2.7 μm) at 50 °C, using a gradient of 0.1% formic acid in water (A) and acetonitrile (B) at 0.4 mL/min over 17 min. Mass spectrometric detection was carried out using electrospray ionization (ESI) in both positive and negative ion modes (40 - 1,700 m/z for MS1 and 25 - 1,000 m/z for MS2), with collision energies of 10 and 20 eV. Raw data processing and metabolite annotation were conducted using MS-DIAL software (version 5.3). For pure semi-quantitative profiling, mass intensity was normalized to sulfadimethoxine internal standard. Mass exclusions were 121.0509 and 922.0098 m/z for positive ion modes and 112.9856, 119.0363, 966.0007, and 1033.9881 m/z for negative ion modes. In accordance with the Metabolomics Standards Initiative (MSI) guidelines [18,19], peaks were filtered based on the retention time limit of 0.2 - 18 min, sample/blank ratio of > 100, a mass tolerance of ≤ 20 ppm, a signal-to-noise ratio of ≥ 3, and an identification threshold of composite score 0.70. This composite score integrated mass accuracy, isotopic pattern similarity, and MS/MS spectral matching. Putative compound identification was performed by MSI Level 2 based on spectral matching against established databases, including the MS-DIAL ESI (+/-) MS/MS authentic standards, Fiehn/Vaniya natural product, and BMDMS-NP databases.

Network pharmacology analysis

The SMILES strings of albiflorin, oleanolic acid, vitexin, isovitexin, acetyl-vitexin, and agnuside were obtained from PubChem (https://pubchem.ncbi.nlm.nih.gov/) [20]. These SMILES strings were then used to predict the target proteins in SwissTargetPrediction (https://www.swisstargetprediction.ch/; 3/4/2026) [21]. The keyword "liver oxidative stress" was searched in GeneCards: The Human Gene Database (https://www.genecards.org/; 2/4/2026) [22,23]. The target protein of each compound was individually intersected with the top 100 proteins ranked by relevance score from GeneCards: The Human Gene Database using a Venn diagram (https://bioinfogp.cnb.csic.es/tools/venny/) [24]. The intersected proteins were then analyzed for protein-protein interaction networks and Gene Ontology functional annotation by STRING version 12.0 (https://string-db.org/; 5/4/2026) [25].

Statistical analysis

Each biological experiment was performed with three independent biological replicates (n = 3). Data are presented as mean ± standard deviation (SD). One-way ANOVA was performed using GraphPad Prism 11 (GraphPad Software, USA). Multiple comparisons were conducted using Dunnett's test. A p-value < 0.05 was considered statistically significant.

Results and discussion

Cytotoxicity

The liver and kidneys are major organs involved

in the metabolism and elimination of foreign compounds and are therefore particularly vulnerable to damage caused by pharmacologically active substances [26]. In this study, the cytotoxicity of GOE was evaluated in Vero and HepG2 cells to identify a suitable concentration range for subsequent experiments. In Vero cells, GOE did not significantly affect cell viability at concentrations of 200 - 400 µg/mL after 24 h (**Figure 2(A)**), 48 h (**Figure 2(B)**), and 72 h (**Figure 2(C)**) of treatment compared with the control. In HepG2 cells, no significant reduction in cell viability was observed at concentrations of 100 - 300 µg/mL after 24 h (**Figure 2(D)**), 100 - 200 µg/mL after 48 h (**Figure 2(E)**), and 100 µg/mL after 72 h (**Figure 2(F)**), compared with the control. Based on these results, GOE showed no cytotoxic effect in either Vero or HepG2 cells at concentrations below 100 µg/mL across all treatment periods. Therefore, concentrations within this range at 24 h of incubation were considered safe and were selected for further experiments.

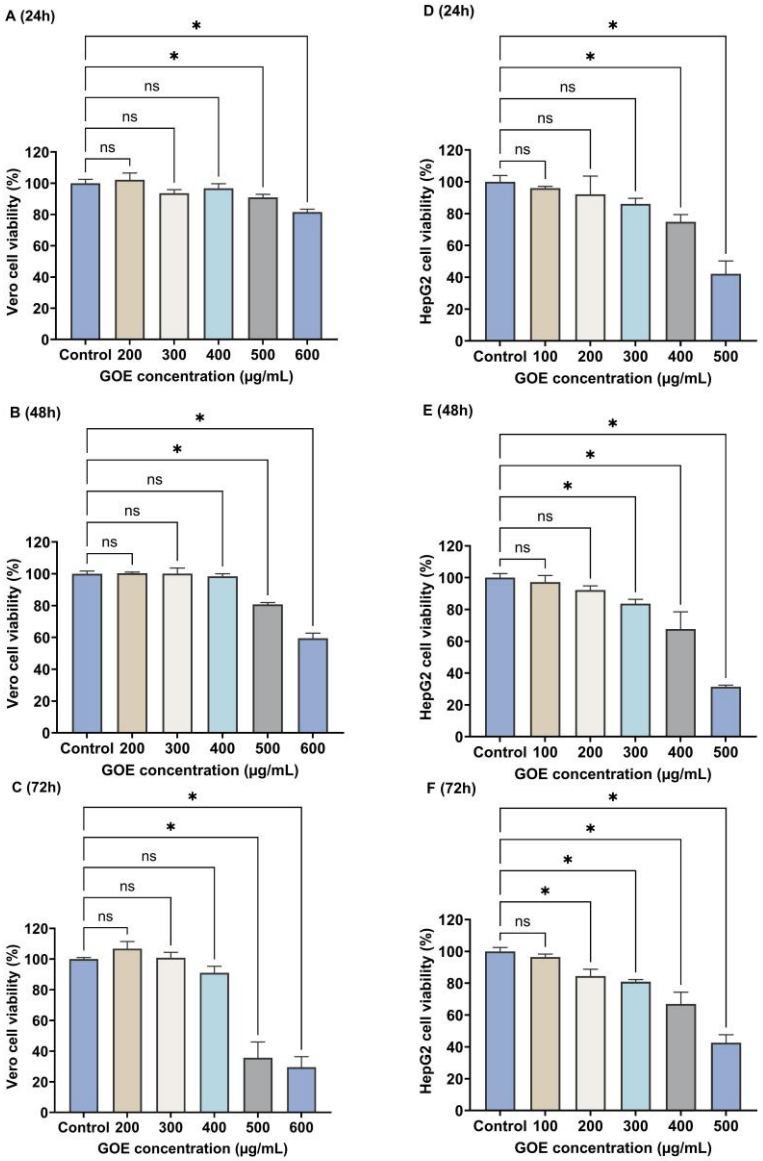


Figure 2 Cytotoxicity of GOE in Vero and HepG2 cells. Cell viability of Vero cells at 24 (A), 48 (B), and 72 h (C) of treatment, and cell viability of HepG2 cells at 24 h (D), 48 h (E), and 72 h (F) of treatment. Vero and HepG2 cells were treated with GOE at concentrations of 0 - 600 and 0 - 500 µg/mL, respectively. Values are presented as mean ± SD. The asterisk (*) indicates a significant difference at $p < 0.05$ compared with the control according to Dunnett's test. ns indicates no significant difference (n = 3).

Protective effect of GOE against H_2O_2-induced oxidative stress in HepG2 cells

Oxidative stress results from an imbalance between oxidants and the antioxidant defense system, leading to excessive production of ROS and reactive nitrogen species (RNS). By reacting with DNA, proteins, and lipids, these reactive species cause cellular damage and contribute to the pathogenesis of various diseases, including liver disease, diabetes, and neurodegenerative disorders [1]. The liver is particularly vulnerable to oxidative stress because it plays a central role in the metabolism of nutrients, xenobiotics, drugs, and alcohol [27]. Due to its metabolic activity and biotransformation processes, the liver is continuously exposed to ROS. Excessive ROS can impair hepatic function, activate inflammatory signaling, and promote the progression of liver injury [2].

In the present study, treatment with H_2O_2 alone significantly reduced cell viability to approximately 81%, compared with 100% of control, indicating that H_2O_2 can induce oxidative stress and damage in HepG2 cells. In contrast, pretreatment with GOE at 3.125 - 25 µg/mL significantly increased cell viability in a concentration-dependent manner (**Figure 3(A)**) compared with H_2O_2-treated cells without GOE pretreatment, suggesting attenuation of H_2O_2-induced oxidative stress and damage. However, pretreatment with GOE at 50 µg/mL resulted in significantly lower cell viability than that observed at 3.125 - 25 µg/mL. This might be due to the biphasic effect of the extract [28]. This result suggests that GOE exhibited its strong protective effect within a concentration range of 6.25 - 25 µg/mL.

Intracellular ROS levels showed a pattern consistent with the cell viability results. In the H_2O_2-treated cells without GOE pretreatment, ROS levels increased significantly to 155.24% compared with the control (**Figure 3B**). Pretreatment with GOE at 3.125 - 25 µg/mL reduced ROS levels in a concentration-dependent manner to 140.71% - 120.72% compared with H_2O_2-treated cells without GOE pretreatment. Although GOE at 50 µg/mL still reduced ROS levels compared with H_2O_2-treated cells, the reduction was less pronounced than that observed at 3.125 - 25 µg/mL. These results further support that GOE was more effective within this tested range.

The fluorescence microscopy images of DCFH-DA staining were in agreement with the quantitative ROS data and cell viability results. Stronger fluorescence intensity was observed in H_2O_2-treated cells without GOE pretreatment than in the control group, indicating increased intracellular ROS accumulation. In contrast, fluorescence intensity was clearly reduced in cells pretreated with GOE at 3.125 - 25 µg/mL (**Figure 3(C)**).

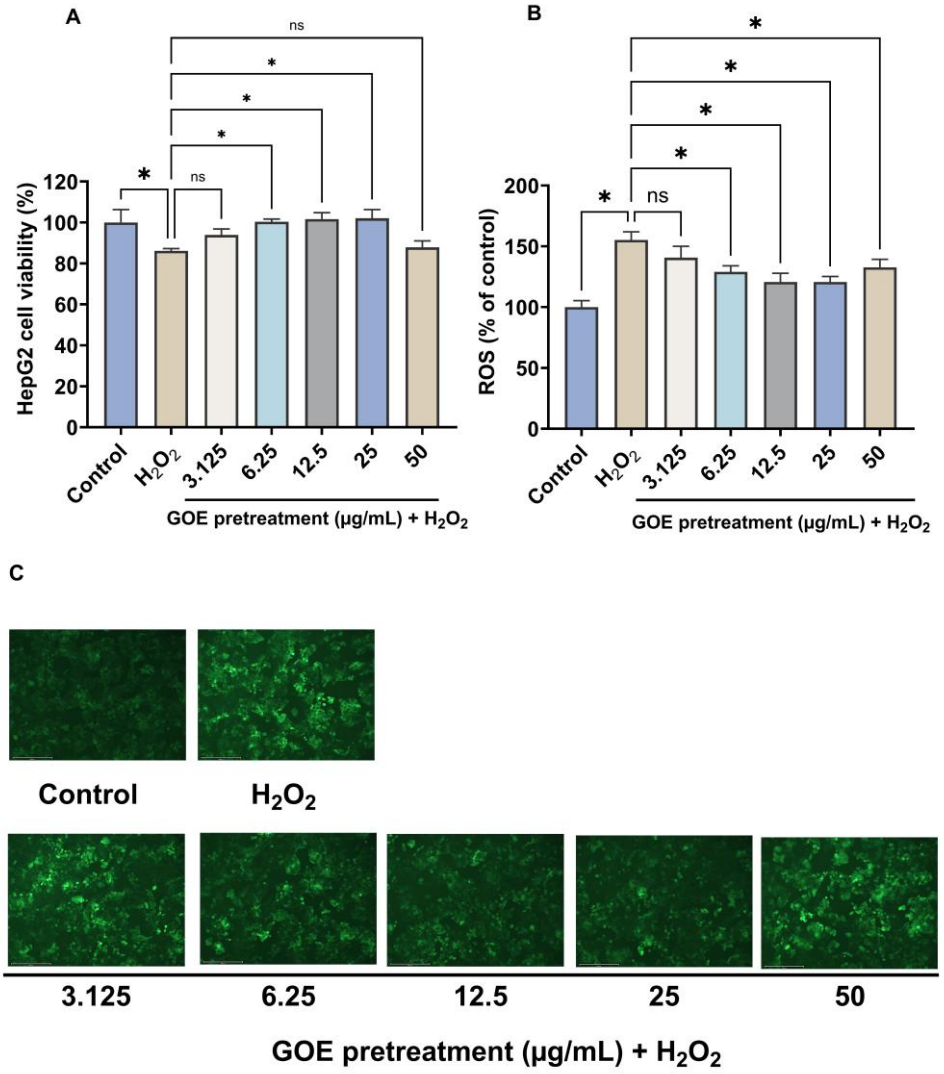


Figure 3 Protective effect of GOE against H_2O_2-induced oxidative stress in HepG2 cells. (A) Cell viability, (B) intracellular ROS levels, and (C) DCFH-DA staining. HepG2 cells were pretreated with GOE at concentrations of 3.125 - 50 μg/mL and subsequently treated with 1 mM H_2O_2. Values are represented as mean ± SD. The asterisk (*) indicates a significant difference at $p < 0.05$ with the H_2O_2-treated cells according to Dunnett's test. ns indicates no significant difference (n = 3).

Hydrogen peroxide (H_2O_2) is one of the major ROS involved in oxidative stress and cellular damage and is widely used to induce oxidative stress in cell models [29,30]. Previous studies have shown that the methanolic extract of *G. oppositifolius* possesses strong antioxidant activity against $O_2^{\cdot}$, OH·, H_2O_2, NO·, and peroxyl radicals [31]. This activity has been associated with the presence of antioxidant phytochemicals, including alkaloids, tannins, flavonoids, saponins, and steroids [13]. In addition, the hepatoprotective effect of methanolic extracts of *G. oppositifolius* has been reported in paracetamol-induced liver damage in rats [32]. In the present study, GOE pretreatment showed a protective effect against H_2O_2-induced oxidative stress and cellular damage in HepG2 cells. These results suggest that GOE may have protective potential in a liver-related *in vitro* model, although further validation in normal hepatocytes or *in vivo* models is required.

GOE inhibits LPS-induced RAW 264.7 cell inflammation

Lipopolysaccharide, a major structural component of the outer membrane of most gram-negative bacteria, is a well-known inducer of inflammation through the

TLR4–MD2 complex. The activation ultimately promotes the production of pro-inflammatory cytokines and chemokines, including IL-1β, IL-6, IL-8, and TNF-α, which accelerate the inflammatory process and stimulates the production of ROS and reactive nitrogen species (RNS) [33]. Elevated LPS levels have also been associated with hepatocyte damage and activation of hepatic macrophages, which further increase pro-inflammatory cytokine production and oxidative stress in the liver [5,6]. Anti-inflammatory activity of GOE was shown in **Figure 4**.

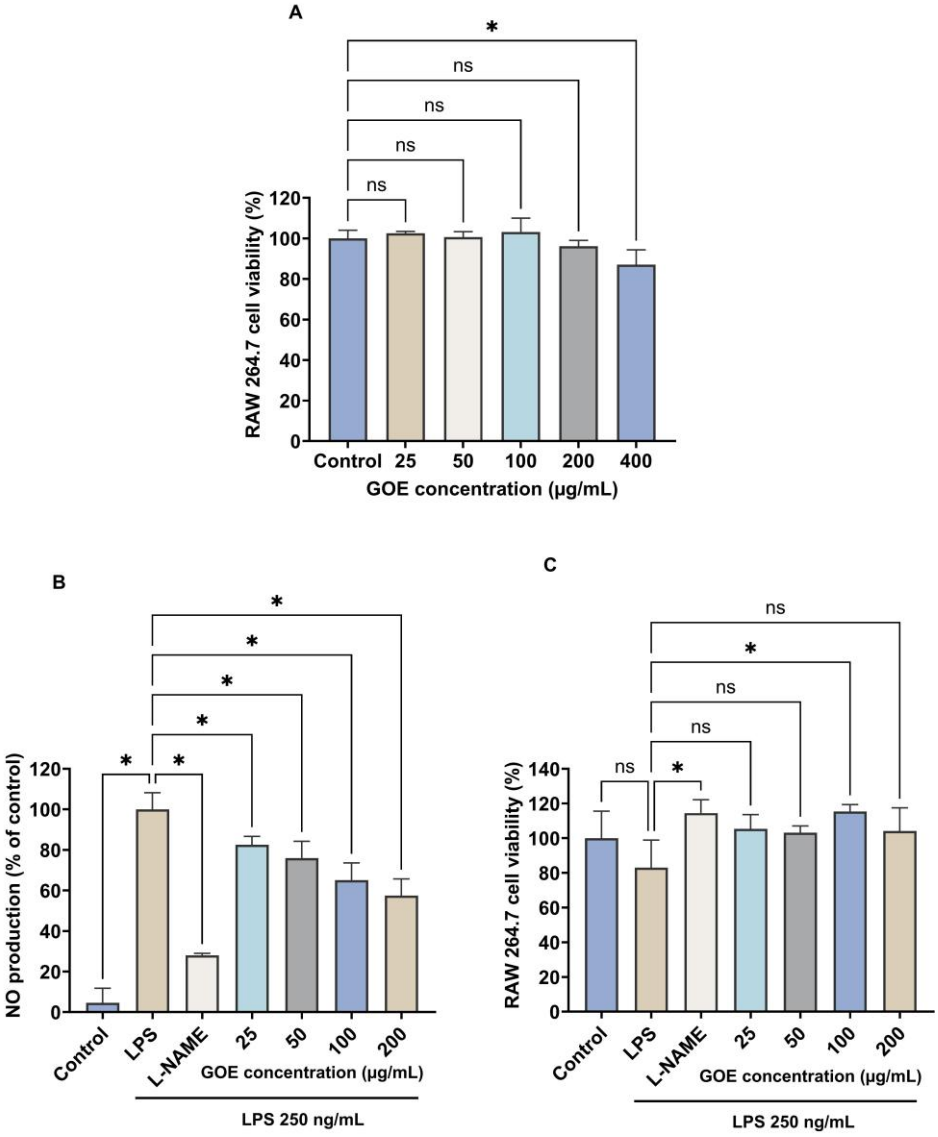


Figure 4 Cytotoxicity and anti-inflammatory activity of GOE in RAW 264.7 cells. (A) Cell viability of RAW 264.7 cells treated with GOE, (B) NO production in LPS-induced RAW 264.7 cells, and (C) cell viability of RAW 264.7 cells treated with GOE. Cells were treated with GOE at concentrations of 25 - 200 μg/mL. Values are represented as mean ± SD. The asterisk (*) indicates a significant difference at $p < 0.05$ with the control and LPS-treated cells for cytotoxicity and anti-inflammatory activity, respectively, according to Dunnett's test. ns indicates no significant difference (n = 3).

GOE at concentrations of 25 - 200 μg/mL reduced NO production to 82.56% - 57.49% relative to LPS-treated cells (**Figure 4(B)**). This concentration range did not show cytotoxicity toward RAW 264.7 cells (**Figure 4(A)**). In addition, cell viability increased to 114.49% - 104.09% relative to the LPS-treated cells, suggesting the protective effect against LPS-induced inflammation in RAW 264.7 cells (**Figure 4(C)**). These results

demonstrate that GOE exhibits anti-inflammatory activity in LPS-stimulated RAW 264.7 cells and support the potential of Thai-grown *G. oppositifolius* as a promising agent for preventing LPS-induced inflammation.

The anti-inflammatory activity of *G. oppositifolius* extracts has been documented in plants collected from several regions, including Taiwan, Bangladesh, and Mali [11,14,34,35]. Triterpenoids (Spergulagenin B, C, and D), flavonoids (kaempferol, 6, 8-dimethyl-5, 7, 4′-trihydroxyflavone, 5,7-dihydroxy-6,8-dimethylflavone, and 5,4′-dihydroxy-7-methoxy-6,8-dimethylflavone), and aromatics (4-hydroxybenzoic acid, 4-hydroxybenzaldehyde, 4-hydroxyacetophenone, methyl 4-hydroxybenzoate, p-anisic acid, vanillin, 4-hydroxy-3-methoxyacetophenone, acetosyringone, 4-hydroxy-3,5-dimethoxybenzaldehyde, 4-hydroxybenzyl alcohol, 2-(4-hydroxyphenyl)ethanol, cinnamic acid, and trans-ferulic acid) have been reported as anti-inflammatory constituents of *G. oppositifolius* [14].

LC-QTOF-MS results

LC-QTOF-MS-based metabolomic analysis is a powerful and robust tool for phytochemical profiling because it provides accurate mass measurement with high resolution for metabolite identification in plant extracts [36]. Therefore, GOE was profiled using LC-QTOF-MS to obtain an overview of its phytochemical composition. The analysis showed that GOE contained a diverse range of metabolites detected in both positive and negative ion modes. In the positive mode, terpenoids and saponins were the predominant groups, accounting for 53%, followed by phenylpropanoids and flavonoids at 23% (**Figure 5(A)**). In the negative mode, phenylpropanoids and flavonoids were the major groups, accounting for 26.2%, followed by lipids and fatty acyls at 24.5% (**Figure 5(B)**).

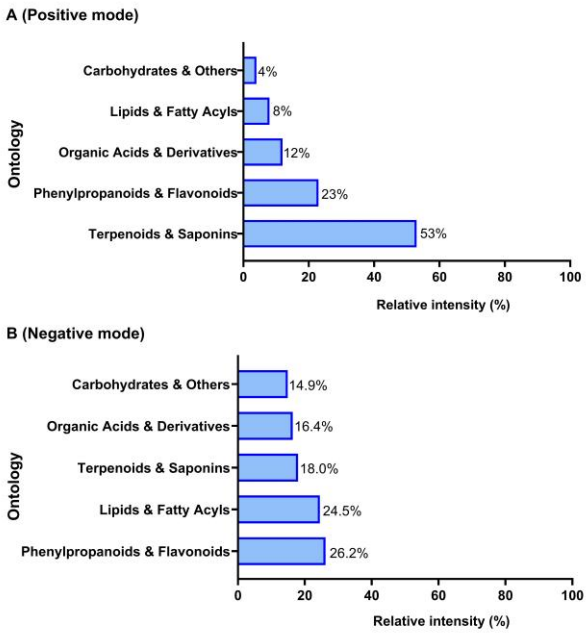


Figure 5 LC-QTOF-MS metabolite distribution in GOE. Relative intensity of tentative metabolites in GOE in (A) positive mode and (B) negative mode of LC-QTOF-MS.

Overall, terpenoids, saponins, phenylpropanoids, and flavonoids appeared to be the major phytochemical constituents in GOE. This finding is consistent with previous reports, showing that triterpenoids and saponins are among the main bioactive compounds in *G. oppositifolius* [14,37-39]. Flavonoid glycosides have also been reported as the predominant phytochemicals in this plant [12,13]. When individual metabolites were considered, the tentative compounds with higher relative intensity were interpreted as being present in greater proportions in the extract (**Table 2**).

Table 2 LC-MS data in positive ion mode for the top 10 tentatively identified compounds in GOE.

Retention Time (min)	Tentative Identification	Ontology	Adduct type	Formula	Observed (m/z)	Relative intensity (%)
1.331	Phenylpropanoid derivative	Anisoles	$[M+Na]^+$	$C_{12}H_{16}O_3$	231.09166	1.03
1.389	Phenylethanolamine	Aralkylamines	$[M+H-H_2O]^+$	$C_8H_{11}NO$	120.08095	1.37
1.661	2-Methylpyrrolidine	Pyrrolidines	$[M+H]^+$	$C_5H_{11}N$	86.09780	1.30
1.683	Isoleucine	Isoleucine and derivatives	$[M+H]^+$	$C_6H_{13}NO_2$	132.10298	1.19
4.191	N-trans-Cinnamoyltyramine	Cinnamamides	$[M+H]^+$	$C_{17}H_{23}NO_4$	306.17099	1.13
4.903	Vitexin	Flavonoid C-glycosides	$[M+H]^+$	$C_{21}H_{20}O_{10}$	433.11887	1.65
4.947	Phenylpropanoid amide	Alkaloids/Phenylpropanoid amides	$[M+H]^+$	$C_{17}H_{23}NO_4$	306.17447	1.21
5.056	Isovitexin	Flavonoid C-glycosides	$[M+H]^+$	$C_{21}H_{20}O_{10}$	433.1178	1.45
5.549	Albiflorin	Terpene glycosides	$[M+K]^+$	$C_{23}H_{28}O_{11}$	519.12238	2.32
8.348	Oleanolic acid	Triterpenoids	$[M+H-H_2O]^+$	$C_{30}H_{48}O_3$	439.36539	1.99

Table 3 LC-MS data in negative ion mode for the top 10 tentatively identified compounds in GOE.

Retention Time (min)	Tentative Identification	Ontology	Adduct type	Formula	Observed (m/z)	Relative intensity (%)
3.556	Agnuside	Iridoid glycosides	$[M-H]^-$	$C_{22}H_{26}O_{11}$	465.1445	1.96
4.261	Agnuside isomer	Iridoid glycosides	$[M-H]^-$	$C_{22}H_{26}O_{11}$	465.14978	3.55
4.909	Vitexin	Flavonoid C-glycosides	$[M-H]^-$	$C_{21}H_{20}O_{10}$	431.10318	4.16
5.206	Isovitexin	Flavonoid C-glycosides	$[M-H]^-$	$C_{21}H_{20}O_{10}$	431.10391	2.63
5.513	Unknown Nitrogenous Compound	Organoheterocyclic compounds (Purine-like derivatives)	$[M-H]^-$	$C_{23}H_{22}N_4O_6$	449.15231	3.24
5.655	6"-O-acetylvitexin	Flavonoid C-glycosides	$[M-H]^-$	$C_{23}H_{22}O_{11}$	473.11346	5.02
6.109	Glucose/Galactose derivative	Carbohydrates	$[M-H]^-$	$C_6H_{10}O_5$	161.04651	1.27
7.265	Unknown Nitrogenous Compound	Organic nitrogen compounds	$[M-H]^-$	$C_{38}H_{52}N_6O_7$	703.37439	1.54
10.963	Unknown Nitrogenous Metabolite	Cyclopeptide alkaloids	$[M-H]^-$	$C_{38}H_{50}N_6O_5$	669.36829	1.13
12.693	Unknown Sulfur-containing Metabolite	Sulfur-containing peptides (Thiopeptides)	$[M-H]^-$	$C_{31}H_{44}N_2O_5S$	555.28882	1.73

In the positive mode, albiflorin showed the highest relative intensity, followed by oleanolic acid, vitexin, and isovitexin (**Table 2**). In the negative mode, acetyl-vitexin showed the highest relative intensity, followed by vitexin, agnuside, and isovitexin (**Table 3**). The detection of vitexin is in agreement with the report of Sahakitpichan *et al.* [40]. These results suggest that these tentative metabolites are relevant to the development of standardized extraction protocols. Reactive oxygen species are key mediators of apoptotic cell death in liver diseases [2]. Among the phytochemicals tentatively annotated in GOE, flavonoids are particularly relevant because they are well known for their free radical scavenging abilities. Their multiple hydroxyl groups facilitate the neutralization of ROS, thereby reducing oxidative stress within the cellular environment [41]. The high abundance of saponins appeared to correlate with the anti-inflammatory properties. These compounds are known to inhibit pro-inflammatory mediators and

downregulate inflammatory cytokines [14,42].

Overall, LC-QTOF-MS results indicate that GOE contains a chemically diverse phytochemical profile, and major annotated metabolites are likely to contribute to its biological activity. To further investigate the protective mechanism of GOE, the compounds with the top three relative intensities in each mode, along with their clear tentative identifications, including albiflorin, oleanolic acid, vitexin, isovitexin, acetyl-vitexin, and agnuside, were selected for subsequent network pharmacology analysis.

Network pharmacology

The target proteins of albiflorin, oleanolic acid, vitexin, isovitexin, acetyl-vitexin, and agnuside were predicted using SwissTargetPrediction [43]. For each compound, the predicted targets were individually intersected with the list of top 100 proteins by relevance score under the keyword "liver oxidative stress" in GeneCards: The Human Gene Database (**Figure 6**). The intersected proteins are listed in **Table 4**.

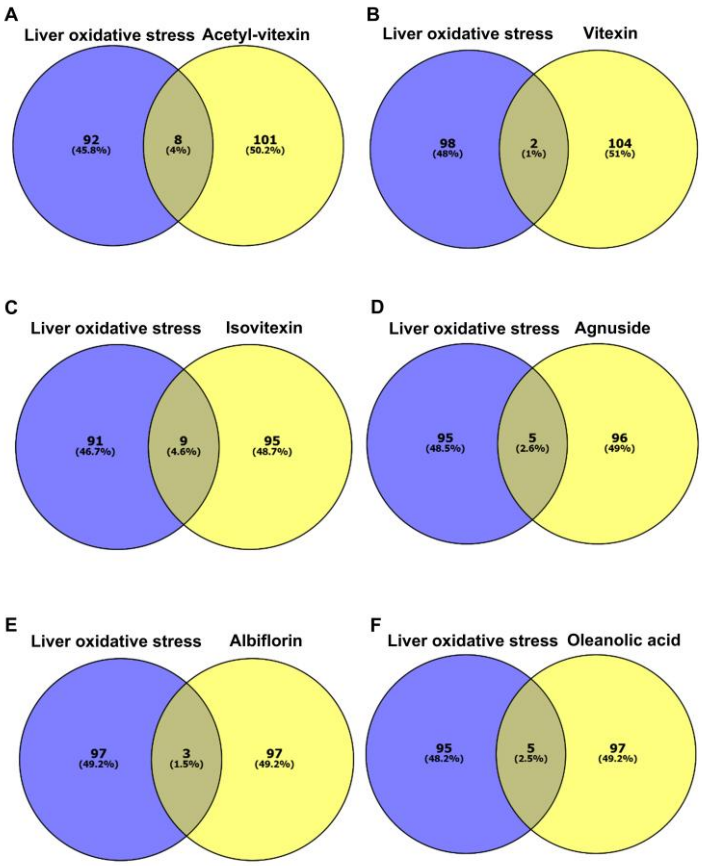


Figure 6 Venn diagrams showing the overlap between liver oxidative stress-related proteins and the predicted target proteins of (A) acetyl-vitexin, (B) vitexin, (C) isovitexin, (D) agnuside, (E) albiflorin, and (F) oleanolic acid.

Table 4 Predicted target proteins of the major annotated metabolites identified in GOE.

Metabolite names	Target proteins
Acetyl-vitexin	TP53, TNF, CTNNB1, SIRT1, AKT1, HIF1A, VEGFA, PIK3CA
Vitexin	MAPK8, PIK3CA
Isovitexin	TP53, TNF, AKT1, PPARG, HIF1A, PTGS2, XDH, EGFR, CFTR
Agnuside	TNF, CASP3, MAPK1, CASP8, PIK3CA
Albiflorin	HSPA5, VEGFA, EGFR
Oleanolic acid	NOS2, IL6, PPARG, PTGS2, TERT

The intersected proteins were then analyzed for protein-protein interactions using STRING version 12.0, and the resulting network is shown in **Figure 7**. The top 10 results of the functional enrichment analysis of the target proteins are presented in **Figures 8** and **9**. The biological processes, molecular functions, cellular components, and KEGG pathways identified in the enrichment analysis suggested that the target proteins were potentially involved in apoptosis.

Moreover, the protein-protein interaction network was further clustered using DBSCAN, a method that identifies clusters based on local node density. Two major clusters were identified, specifically, an apoptosis-related protein cluster associated with the regulation of HMOX1 expression and activity cluster, and these two clusters interacted with each other (**Figure 7**). Since regulation of HMOX1 expression and activity is closely linked to the Nrf2-ARE pathway [7], these findings suggest that GOE may provide its protective effect by suppressing apoptosis and modulating the Nrf2-ARE pathway.

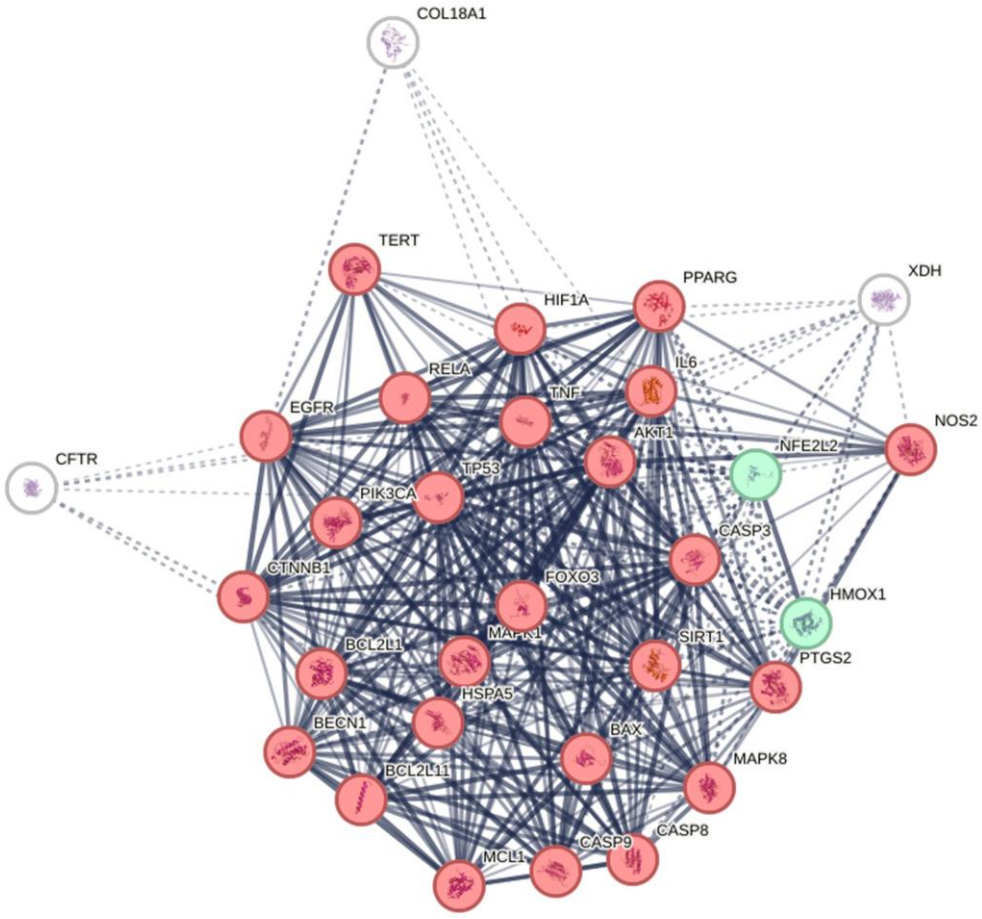


Figure 7 Protein-protein interactions and KEGG pathways analysis. The network was clustered using DBSCAN in STRING based on local node density. The red and green circles represent the apoptosis-related protein cluster associated with the regulation of HMOX1 expression and activity cluster, respectively.

Previous reports show that the high concentrations of antioxidant-rich phenolics in the extract have been associated with activation of Nrf2 translocation into the nucleus. Once in the nucleus, Nrf2 binds to the antioxidant response element (ARE) in the promoter region of various cytoprotective genes. The upregulation of the Nrf2-ARE pathway leads to the increased expression of endogenous antioxidant enzymes, which can neutralize oxidative stress in the liver and provide a protective effect [44-48].

Among the major metabolites tentatively annotated in GOE, albiflorin, a monoterpene glycoside,

has been reported to exhibit anti-inflammatory and anti-apoptotic activities and to activate the Nrf2-HO-1 pathway [49,50]. Oleanolic acid is also well known for its protective effect against oxidative stress [51,52]. Information on the protective effect of acetyl-vitexin against oxidative stress remains limited, whereas vitexin and isovitexin have been more widely reported to exert anti-oxidative stress and anti-apoptotic effects through activation of the Nrf2-ARE signaling pathway [53]. Agnuside has also been reported to provide anti-inflammatory, analgesic, anticancer, and antioxidant activities [54,55].

Based on the literature, network pharmacology, and LC-QTOF-MS results, a significant proportion of albiflorin, oleanolic acid, vitexin, isovitexin, acetyl-vitexin, and agnuside are likely candidate contributors to the biological activity of GOE, possibly associated with Nrf2-ARE and apoptosis-related pathways.

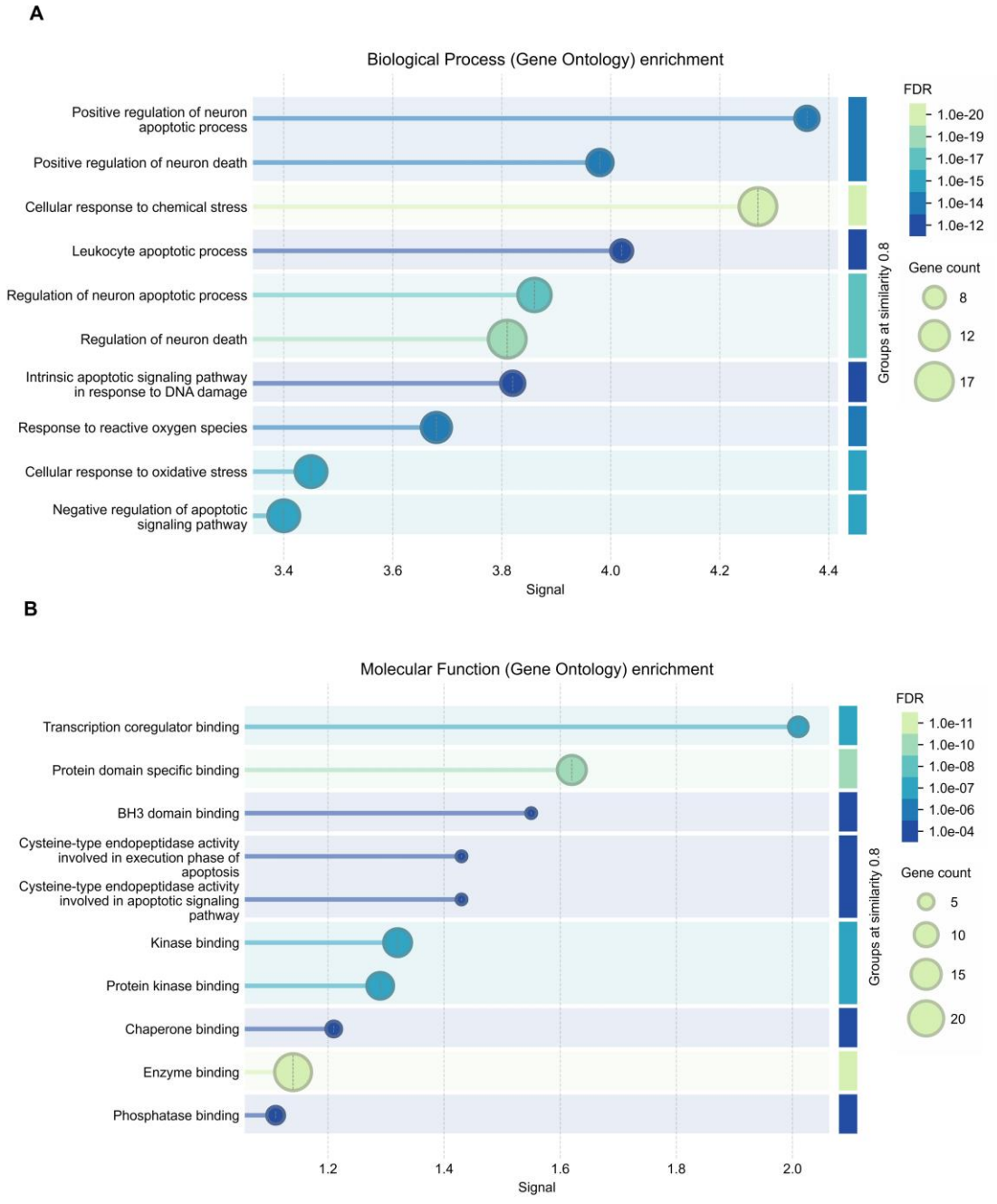


Figure 8 Gene-ontology (GO) functional annotation generated by STRING: (A) biological process and (B) molecular function.

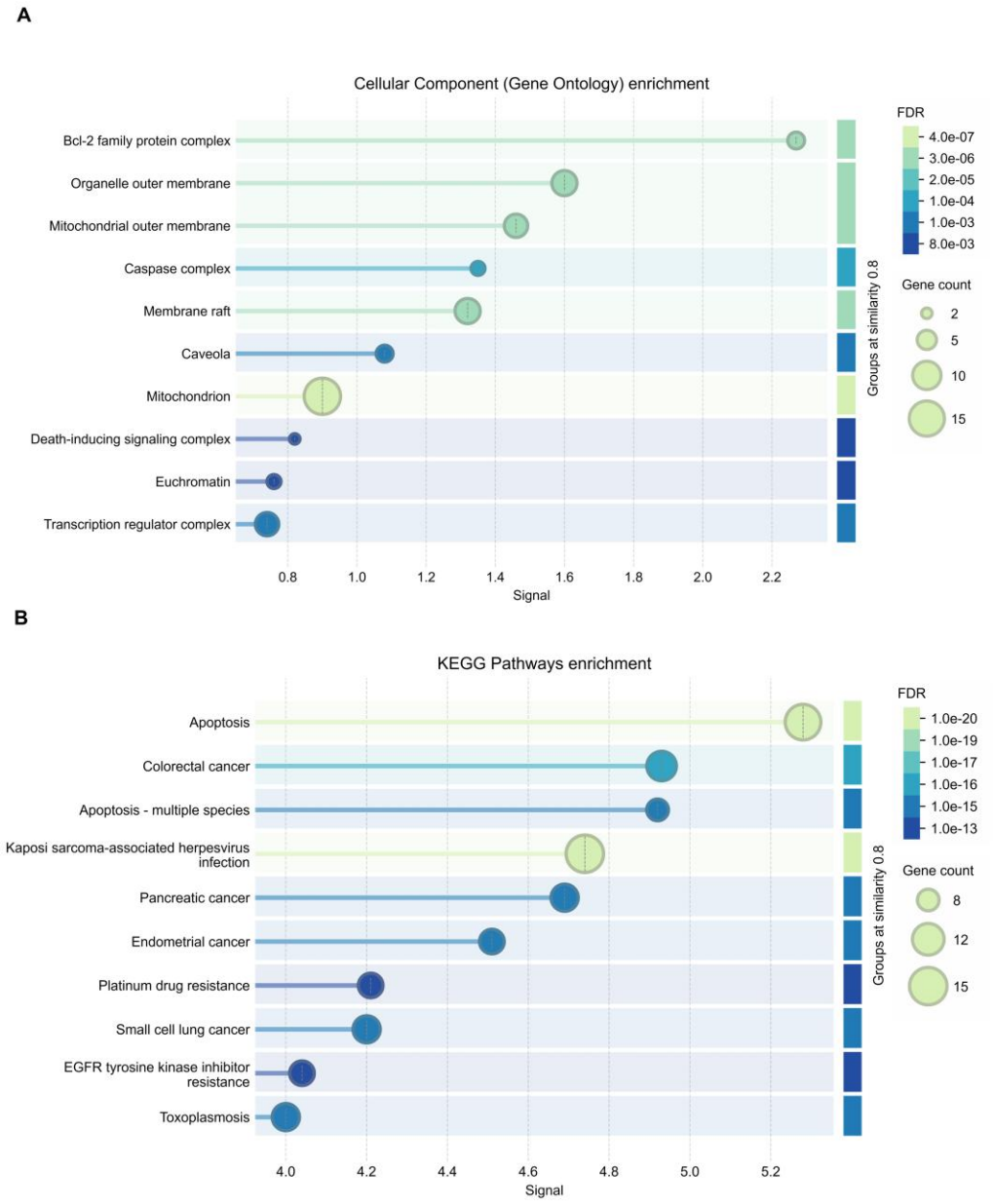


Figure 9 Gene-ontology (GO) functional annotation generated by STRING: (A) cellular component and (B) KEGG pathways.

Gene expression

Network pharmacology analysis suggested that the protective effect of GOE may be associated with modulation of the Nrf2-ARE pathway and apoptosis. Therefore, the expression of genes related to apoptosis (**Figure 10**) and the Nrf2-ARE pathway was further examined (**Figure 11**).

TNF-α is a primarily pro-inflammatory cytokine that can participate in apoptosis signaling [27] and promote apoptosis through the TNF Receptor [56]. In addition, the tumor suppressor protein p53 transcriptionally upregulates pro-apoptotic genes such as PUMA, Noxa, and Bax, while directly downregulating anti-apoptotic genes such as Bcl-2, causing mitochondrial outer membrane permeabilization and subsequent release of cytochrome c. The release of cytochrome c activates the Caspase-9/3 proteolytic cascade, executing the programmed cell death [57]. In the present study, H_2O_2 treatment without GOE pretreatment increased the mRNA expression of TNF-α, P53, Bax, and Casp3, whereas the mRNA expression of the anti-apoptotic gene Bcl-2 was

decreased. These results indicate that H_2O_2 induced apoptosis in HepG2 cells. In contrast, pretreatment with GOE suppressed the mRNA expression of TNF-α, P53, Bax, and Casp3, while increasing Bcl-2 mRNA expression compared with H_2O_2-treated cells without GOE pretreatment (**Figure 10**). This implied that GOE protected HepG2 cells by modulating apoptosis.

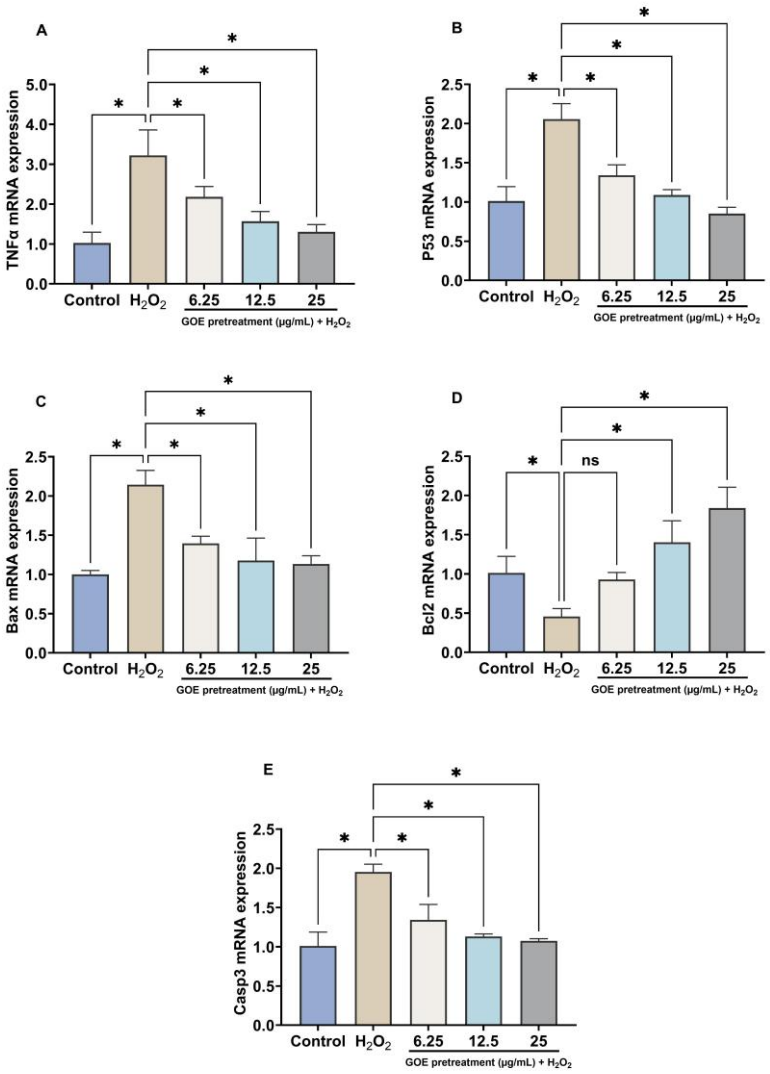


Figure 10 Gene expression of apoptosis-associated genes in H_2O_2-treated cells with and without GOE pretreatment at concentrations of 6.25 - 25 µg/mL: (A) TNF-α, (B) TP53, (C) Bax, (D) Bcl-2, and (E) Casp3. Values are represented as mean ± SD. The asterisk (*) indicates a significant difference at $p < 0.05$ with the control according to Dunnett's test. ns indicates no significant difference (n = 3).

The Nrf2-ARE pathway plays a central role as the defense mechanism against oxidative stress in the liver. Under oxidative stress conditions, the transcription factor Nrf2 dissociates from its inhibitory protein, Keap1, and translocates into the nucleus, where it binds to the ARE, resulting in the up-regulation of antioxidant enzymes, such as superoxide dismutase (SOD), catalase (CAT), heme oxygenase-1 (HO-1), and NAD(P)H:quinone oxidoreductase 1 (NQO1). These enzymes effectively neutralize excessive ROS in the liver [58]. In addition, activation of the Nrf2-ARE pathway plays a critical role in inhibiting apoptosis-induced cell death [59].

In this study, H_2O_2-treated cells without GOE pretreatment decreased the mRNA expression of Nrf2 and antioxidant enzyme genes (SOD, CAT, HO-1, and NQO1) and increased Keap1, indicating that H_2O_2 disrupted the antioxidant system of HepG2 cells by

modulating the Nrf2-ARE pathway. In contrast, GOE pretreatment reduced Keap1 mRNA expression and increased the mRNA expression of Nrf2, SOD, CAT, HO-1, and NQO1, as compared with H_2O_2-treated cells without GOE pretreatment (**Figure 11**). SOD acts as the first-line antioxidant enzyme by catalyzing the dismutation of superoxide radicals into H_2O_2 [60], which is then rapidly decomposed into water and oxygen by CAT [61]. HO-1 degrades free heme and promotes iron sequestration by ferritin, thereby preventing the production of hydroxyl radical from the Fenton reaction between H_2O_2 and heme [62]. NQO1 catalyzes the reduction of reactive quinones and helps prevent additional endogenous H_2O_2 production [63,64]. Therefore, the upregulation of these antioxidant enzymes indicated that GOE pretreatment effectively mitigated oxidative stress by modulating the Nrf2-ARE pathway, directly scavenging H_2O_2 via SOD and CAT, and suppressing further generation of endogenous H_2O_2 and other ROS through HO-1 and NQO1. This finding is consistent with the important role of Nrf2 in preventing and limiting oxidative stress in the liver [65,66].

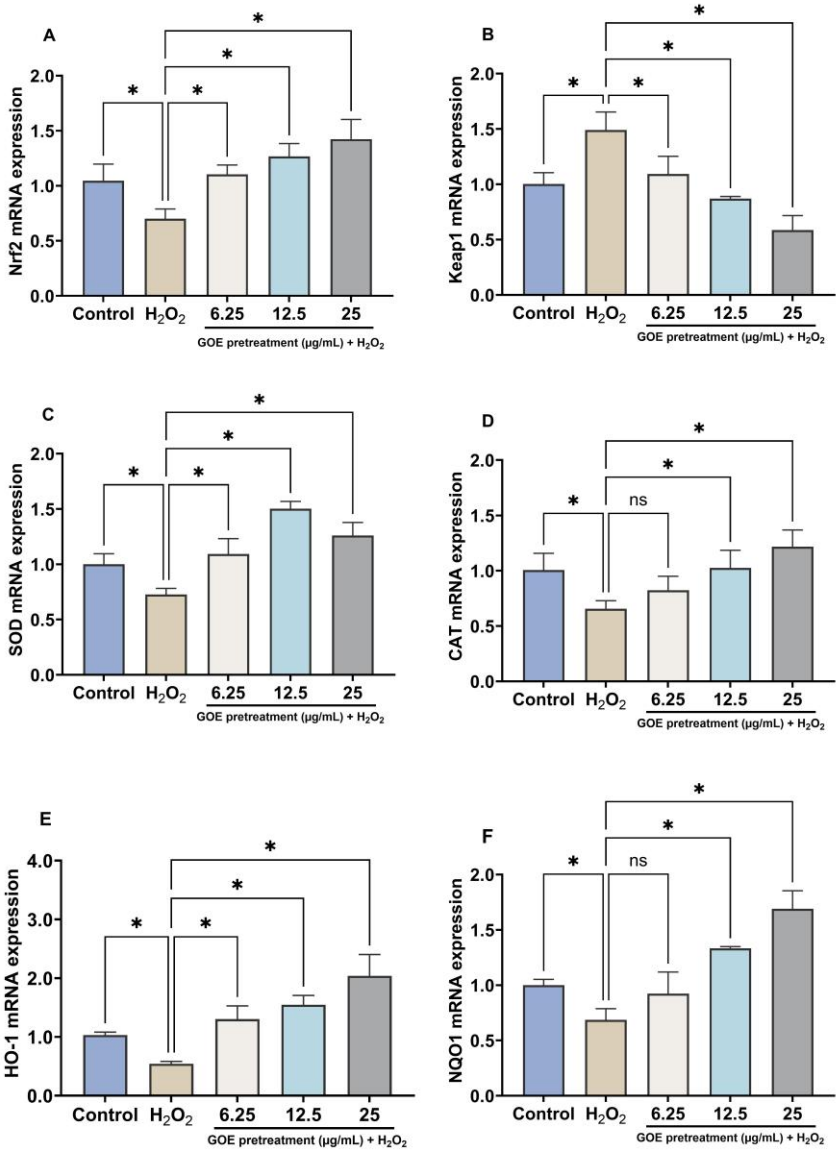


Figure 11 Gene expression. (A) Nrf2, (B) Keap1, (C) SOD, (D) CAT, (E) HO-1, and (F) NQO1 of H_2O_2-treated cells with and without GOE pretreatment ranging from 6.25 - 25 μg/mL. The values are represented as mean ± SD. The asterisk (*) indicates a significant difference at $p < 0.05$ with the control according to Dunnett's test. ns indicates no significant difference (n = 3).

Overall, the gene expression results showed that GOE exerted a protective effect against H_2O_2-induced oxidative stress and cellular damage by activating the Nrf2-ARE pathway, resulting in increased antioxidant enzymes, reduced oxidative stress, and inhibition of apoptotic cell death. The gene expression findings agreed with the network pharmacology results and highlighted the hepatoprotective effect of GOE, supporting its potential for pharmaceutical investigation.

Conclusions

GOE pretreatment showed protective effects in HepG2 cells by reducing intracellular ROS production. GOE also exhibited anti-inflammatory activity in LPS-induced RAW 264.7 cells. Metabolomic analysis showed that GOE contained a diverse range of bioactive metabolites, with phenylpropanoids, flavonoids, terpenoids, and saponins as the major phytochemical groups. Network pharmacology and gene expression analyses suggested that the protective effect of GOE was associated with modulation of the Nrf2-ARE signaling pathway and apoptosis. Albiflorin, oleanolic acid, vitexin, isovitexin, acetyl-vitexin, and agnuside may be candidate contributors to the protective effect of GOE. Real-time PCR further suggested that GOE suppressed apoptosis by downregulating TNF-α, P53, Bax, and Casp3, while upregulating Bcl-2 gene expression. In addition, GOE modulated the Nrf2-ARE signaling pathway by reducing Keap1 and increasing Nrf2, SOD, CAT, HO-1, and NQO1 gene expression. Overall, these findings indicate that GOE is a promising source of bioactive phytochemicals with protective potential against H_2O_2-induced oxidative stress and damage and may be useful for future pharmaceutical investigation.

Acknowledgements

This work was supported by the Science Achievement Scholarship of Thailand (SAST).

Declaration of generative AI in scientific writing

The authors acknowledge the use of generative AI tools ChatGPT 5.3 Instant and Gemini 3 Flash to assist in the preparation of the graphical abstract and ensure compliance with the journal AI policy. No content generation or data interpretation was performed by AI. The authors take full responsibility for the content and conclusions of this work.

CRediT author statement

Alisa Naladta: Conceptualization, Methodology, Validation, Formal analysis, Investigation, Data Curation, Visualization, Writing - Original Draft. **Natsajee Nualkaew**: Supervision, Resources, Writing - Review & Editing. **Liudmila Yarovaya**: Validation, Writing - Review & Editing. **Santi Phosri and La-or Somsakeesit**: Resources, Writing - Review & Editing; **Khomsorn Lomthaisong and Anupong Joompang**: Conceptualization, Supervision, Methodology, Resources, Validation, Data Curation.

References

[1] VP Reddy. Oxidative stress in health and disease. *Biomedicines* 2023; **11(11)**, 2925.

[2] A Allameh, R Niayesh-Mehr, A Aliarab, G Sebastiani and K Pantopoulos. Oxidative stress in liver pathophysiology and disease. *Antioxidants* 2023; **12(9)**, 1653.

[3] L Conde de la Rosa, L Goicoechea, S Torres, C Garcia-Ruiz and JC Fernandez-Checa. Role of oxidative stress in liver disorders. *Livers* 2022; **2(4)**, 283-314.

[4] P Banerjee, N Gaddam, V Chandler and S Chakraborty. Oxidative stress-induced liver damage and remodeling of the liver vasculature. *The American Journal of Pathology* 2023; **193(10)**, 1400-1414.

[5] Y Zhou, X Hu, S Zhong, W Yu, J Wang, W Zhu, T Yang, G Zhao, Y Jiang and Y Li. Effects of continuous LPS induction on oxidative stress and liver injury in weaned piglets. *Veterinary Sciences* 2022; **10(1)**, 22.

[6] K Nakadate, H Saitoh, M Sakaguchi, F Miruno, N Muramatsu, N Ito, K Tadokoro and K Kawakami. Advances in understanding lipopolysaccharide-mediated hepatitis: Mechanisms and pathological features. *Current Issues in Molecular Biology* 2025; **47(2)**, 79.

[7] J Zhou, Q Zheng and Z Chen. The Nrf2 pathway in liver diseases. *Frontiers in Cell and Developmental Biology* 2022; **10**, 826204.

[8] W Tu, H Wang, S Li, Q Liu and H Sha. The anti-inflammatory and anti-oxidant mechanisms of the Keap1/Nrf2/ARE signaling pathway in chronic diseases. *Aging and Disease* 2019; **10(3)**, 637-651.

[9] TX Tee, LT Kee, TT Chai, HC Yam, HM Reza, FC Wong, JX Law and SA Tan. Plant-derived Nrf2 activators to enhance liver antioxidative and regenerative potentials. *Revista Brasileira de Farmacognosia* 2025; **35(1)**, 61-77.

[10] L Zorem, B Bohia, Lalrokimi, R Lalmuanpuii, F Lalremruati, A Fanai, N Lalhriatpuii, C Lalmuansangi, L Tochhawng, H Lalruatsanga, PK Singh and Zothanpuia. Ethnobotanical validation and phytochemical profiling of *Glinus oppositifolius* (L.) Aug. DC used by indigenous tribes of Mizoram. *Discover Food* 2026; **6(1)**, 91.

[11] N Hoque, MR Habib, MZ Imam, J Ahmed and M Sohel. Analgesic and anti-inflammatory potential of methanolic extract of *Glinus oppositifolius* L. *Australian Journal of Basic and Applied Sciences* 2011; **5**, 729-733.

[12] C Das, G Ghosh, G Rath, D Das, B Kar, D Pradhan, VK Rai, TK Rajwar, J Halder and P Dash. Chemometric profiling and anti-arthritic activity of aerial parts of *Glinus oppositifolius* (L.) Aug. DC. *Journal of Ethnopharmacology* 2024; **328**, 117991.

[13] SY Sheu, CH Yao, YC Lei and TF Kuo. Recent progress in *Glinus oppositifolius* research. *Pharmaceutical Biology* 2014; **52(8)**, 1079-1084.

[14] JJ Chen, CS Yang, YH Chen, CY Chao, YC Chen and YH Kuo. New triterpenoids and anti-inflammatory constituents from *Glinus oppositifolius*. *Molecules* 2023; **28(7)**, 2903.

[15] M Feoktistova, P Geserick and M Leverkus. Crystal violet assay for determining viability of cultured cells. *Cold Spring Harbor Protocols* 2016; **2016(4)**, pdb.prot087379.

[16] E García-Pérez, D Ryu, C Lee and HJ Lee. Ochratoxin a induces oxidative stress in HepG2 cells by impairing the gene expression of antioxidant enzymes. *Toxins* 2021; **13(4)**, 271.

[17] KJ Livak and TD Schmittgen. Analysis of relative gene expression data using real-time quantitative PCR and the 2(-Delta Delta C(T)) Method. *Methods* 2001; **25(4)**, 402-408.

[18] LW Sumner, A Amberg, D Barrett, MH Beale, R Beger, CA Daykin, TW Fan, O Fiehn, R Goodacre, JL Griffin, T Hankemeier, N Hardy, J Harnly, R Higashi, J Kopka, AN Lane, JC Lindon, P Marriott, AW Nicholls, MD Reily, JJ Thaden and MR Viant. Proposed minimum reporting standards for chemical analysis Chemical Analysis Working Group (CAWG) Metabolomics Standards Initiative (MSI). *Metabolomics* 2007; **3(3)**, 211-221.

[19] H Tsugawa, T Cajka, T Kind, Y Ma, B Higgins, K Ikeda, M Kanazawa, J VanderGheynst, O Fiehn and M Arita. MS-DIAL: Data-independent MS/MS deconvolution for comprehensive metabolome analysis. *Nature Methods* 2015; **12(6)**, 523-526.

[20] S Kim, J Chen, T Cheng, A Gindulyte, J He, S He, Q Li, BA Shoemaker, PA Thiessen, B Yu, L Zaslavsky, J Zhang and EE Bolton. PubChem 2025 update. *Nucleic Acids Research* 2024; **53(D1)**, D1516-D1525.

[21] D Gfeller, O Michielin and V Zoete. Shaping the interaction landscape of bioactive molecules. *Bioinformatics* 2013; **29(23)**, 3073-3079.

[22] G Stelzer, N Rosen, I Plaschkes, S Zimmerman, M Twik, S Fishilevich, T Iny Stein, R Nudel, I Lieder, Y Mazor, S Kaplan, D Dahary, Y Warshawsky, A Guan-Golan, A Kohn, N Rappaport, M Safran and D Lancet. The GeneCards suite: From gene data mining to disease genome sequence analyses. *Current Protocols in Bioinformatics* 2016; **54(1)**, 1-30.

[23] M Safran, N Rosen, M Twik, R BarShir, TI Stein, D Dahary, S Fishilevich and D Lancet. *The GeneCards suite. In*: I Abugessaisa and T Kasukawa (Eds.). Practical guide to life science databases. Springer Nature, Singapore, 2021, p. 27-56.

[24] JC Oliveros. An interactive tool for comparing lists with Venn's diagrams. Available at: https://bioinfogp.cnb.csic.es/tools/venny/index.html, accessed April 2026.

[25] D Szklarczyk, R Kirsch, M Koutrouli, K Nastou, F Mehryary, R Hachilif, AL Gable, T Fang, NT Doncheva, S Pyysalo, P Bork, LJ Jensen and C von Mering. The STRING database in 2023: Protein-protein association networks and functional

enrichment analyses for any sequenced genome of interest. *Nucleic Acids Research* 2023; **51(D1)**, D638-D646.

[26] H Alothaid. Evaluation of cytotoxicity, oxidative stress and organ-specific effects of activated carbon from Al-Baha date palm kernels. *Saudi Journal of Biological Sciences* 2022; **29(9)**, 103387.

[27] J Lee, J Kim, R Lee, E Lee, TG Choi, AS Lee, YI Yoon, GC Park, JM Namgoong, SG Lee and E Tak. Therapeutic strategies for liver diseases based on redox control systems. *Biomedicine & Pharmacotherapy* 2022; **156**, 113764.

[28] J Jodynis-Liebert and M Kujawska. Biphasic dose-response induced by phytochemicals: Experimental evidence. *Journal of Clinical Medicine* 2020; **9(3)**, 718.

[29] R Jia, J Du, L Cao, Y Li, O Johnson, Z Gu, G Jeney, P Xu and G Yin. Antioxidative, inflammatory and immune responses in hydrogen peroxide-induced liver injury of Tilapia (GIFT, *Oreochromis niloticus*). *Fish & Shellfish Immunology* 2019; **84**, 894-905.

[30] IP Miller, I Pavlović, B Poljšak, D Šuput and I Milisav. Beneficial role of ROS in cell survival: Moderate increases in H_2O_2 production induced by hepatocyte isolation mediate stress adaptation and enhanced survival. *Antioxidants* 2019; **8(10)**, 434.

[31] KA Kumar, MU Maheswari, AT Sivashanmugam, VS Devi, N Subhashini and TK Ravi. Free radical scavenging and antioxidant activities of *Glinus oppositifolius* (carpet weed) using different in vitro assay systems. *Pharmaceutical Biology* 2009; **47(6)**, 474-482.

[32] M Gupta, UK Mazumder, PK Haldar, L Manikandan, GP Senthilkumar and CC Kandar. Hepatoprotective activity of methanol extracts of *Glinus oppositifolius* and *Trianthema decandra* against paracetamol induced liver damage. *Advances in Traditional Medicine* 2007; **7(1)**, 74-78.

[33] MJ Page, DB Kell and E Pretorius. The role of lipopolysaccharide-induced cell signalling in chronic inflammation. *Chronic Stress* 2022; **6**, 24705470221076390.

[34] N Hue, V Thuy, N Thu, V Diep, N Hang, N Van, T Luc, N Thi Van Anh, T Hien and D Ha. Anti-inflammatory activity in RAW 264.7 cells by standardized extracts and the isolated compound from *Glinus oppositifolius*. *IOSR Journal of Pharmacy* 2023; **13(12)**, 17-25.

[35] V Alexandru, A Miron and V Bild. Preliminary research concerning antinociceptive and antiinflammatory effects of two extracts from *Glinus oppositifolius* (L.) Aug. DC. *Revista Medico-Chirurgicala* 2014; **118**, 866-872.

[36] P Phucharoenrak, C Muangnoi and D Trachootham. Metabolomic analysis of phytochemical compounds from ethanolic extract of lime (*Citrus aurantifolia*) peel and its anti-cancer effects against human hepatocellular carcinoma cells. *Molecules* 2023; **28(7)**, 2965.

[37] F Traore, R Faure, E Ollivier, M Gasquet, N Azas, L Debrauwer, A Keita, P Timon-David and G Balansard. Structure and antiprotozoal activity of triterpenoid saponins from *Glinus oppositifolius*. *Planta Medica* 2000; **66(4)**, 368-371.

[38] CY Ragasa, DL Espineli, EH Mandia, MJ Don and CC Shen. A new triterpene from *Glinus oppositifolius*. *Chinese Journal of Natural Medicines* 2012; **10(4)**, 284-286.

[39] S Chhanda, T Muslim and M Rahman. Phytochemical studies on *Glinus oppositifolius* (L.) Aug. DC. *Dhaka University Journal of Science* 2015; **62(1)**, 45-48.

[40] P Sahakitpichan, W Disadee, S Ruchirawat and T Kanchanapoom. L-(-)-(N-trans-cinnamoyl)-arginine, an acylamino acid from *Glinus oppositifolius* (L.) Aug. DC. *Molecules* 2010; **15(9)**, 6186-6192.

[41] K Jomova, SY Alomar, R Valko, J Liska, E Nepovimova, K Kuca and M Valko. Flavonoids and their role in oxidative stress, inflammation, and human diseases. *Chemico-Biological Interactions* 2025; **413**, 111489.

[42] Q Zheng, T Wang, S Wang, Z Chen, X Jia, H Yang, H Chen, X Sun, K Wang, L Zhang and F Fu. The anti-inflammatory effects of saponins from natural herbs. *Pharmacology & Therapeutics* 2025; **269**, 108827.

[43] A Daina, O Michielin and V Zoete. SwissTargetPrediction: Updated data and new features for efficient prediction of protein targets

of small molecules. *Nucleic Acids Research* 2019; **47(W1)**, W357-W364.

[44] W Huang, Y Zhong, B Gao, B Zheng and Y Liu. Nrf2-mediated therapeutic effects of dietary flavones in different diseases. *Frontiers in Pharmacology* 2023; **14**, 1240433.

[45] YR Li, GH Li, MX Zhou, L Xiang, DM Ren, HX Lou, XN Wang and T Shen. Discovery of natural flavonoids as activators of Nrf2-mediated defense system: Structure-activity relationship and inhibition of intracellular oxidative insults. *Bioorganic & Medicinal Chemistry* 2018; **26(18)**, 5140-5150.

[46] A Gugliandolo, P Bramanti and E Mazzon. Activation of Nrf2 by natural bioactive compounds: A promising approach for stroke? *International Journal of Molecular Sciences* 2020; **21(14)**, 4875.

[47] Y Liao, F Lv, T Quan, C Wang and J Li. Flavonoids in natural products for the therapy of liver diseases: Progress and future opportunities. *Frontiers in Pharmacology* 2024; **15**, 1485065.

[48] YN Li, Y Guo, M Xi, P Yang, XY Zhou, S Yin, CX Hai, JG Li and XJ Qin. Saponins from *Aralia taibaiensis* attenuate D-galactose-induced aging in rats by activating FOXO3a and Nrf2 pathways. *Oxidative medicine and cellular longevity* 2014; **2014**, 320513.

[49] H Zhang, J Wang, W Lang, H Liu, Z Zhang, T Wu, H Li, L Bai and Q Shi. Albiflorin ameliorates inflammation and oxidative stress by regulating the NF-κB/NLRP3 pathway in Methotrexate-induced enteritis. *International Immunopharmacology* 2022; **109**, 108824.

[50] C Park, HJ Cha, DG Kim, SH Hong, SK Moon, CY Jin, GY Kim, HS Kim, NY Lee, JH Shim and YH Choi. Albiflorin, a monoterpene glycoside, protects myoblasts against hydrogen peroxide-induced apoptosis by activating the Nrf2/HO-1 axis. *Biomolecules & Therapeutics* 2025; **33(4)**, 716-727.

[51] SA Reisman, LM Aleksunes and CD Klaassen. Oleanolic acid activates Nrf2 and protects from acetaminophen hepatotoxicity via Nrf2-dependent and Nrf2-independent processes. *Biochemical pharmacology* 2009; **77(7)**, 1273-1282.

[52] A Günther and B Bednarczyk-Cwynar. Oleanolic acid: A promising antioxidant-sources, mechanisms of action, therapeutic potential, and enhancement of bioactivity. *Antioxidants* 2025; **14(5)**, 598.

[53] W Yan, J Cheng and B Xu. Dietary flavonoids vitexin and isovitexin: New insights into their functional roles in human health and disease prevention. *International Journal of Molecular Sciences* 2025; **26(14)**, 6997.

[54] BT Lam, HT Ly, HT Tran and VM Le. Investigation of the main active ingredients of Vitex rotundifolia L.f and assessment of their contribution to the activity of this species. *Pharmacological Research - Modern Chinese Medicine* 2025; **15**, 100608.

[55] R Gnanarajan, D Uvarajan, N Ravichandran, PA Karuppusamy, K Krishnamoorthy, B Vellingiri and A Narayanasamy. Agnuside enhances neuronal survival and cognitive function by modulating PI3K/AKT/mTOR signaling in Aluminium Chloride induced Alzheimer's disease. *Progress in Neuro-Psychopharmacology and Biological Psychiatry* 2025; **142**, 111532.

[56] A Guerrache and O Micheau. TNF-related apoptosis-inducing ligand: Non-apoptotic signalling. *Cells* 2024; **13(6)**, 521.

[57] Q Hao, J Chen, H Lu and X Zhou. The ARTS of p53-dependent mitochondrial apoptosis. *Journal of Molecular Cell Biology* 2023; **14(10)**, mjac074.

[58] M Fuertes-Agudo, M Luque-Tévar, C Cucarella, P Martín-Sanz and M Casado. Advances in understanding the role of NRF2 in liver pathophysiology and its relationship with hepatic-specific cyclooxygenase-2 expression. *Antioxidants* 2023; **12(8)**, 1491.

[59] N Li, L Hao, S Li, J Deng, F Yu, J Zhang, A Nie and X Hu. The NRF-2/HO-1 signaling pathway: A promising therapeutic target for metabolic dysfunction-associated steatotic liver disease. *Journal of Inflammation Research* 2024; **17**, 8061-8083.

[60] E Martindah, AR Khairullah, R Widiastuti, A Andriani, R Damayanti, I Mustofa, S Mulyati, M Sukmanadi, BWK Wardhani, RZ Ahmad, AO Akintunde, BP Pratama, I Melati, DAA Kurniasih, ANM Ansori, W Yulianti, M Nirwan and S

Wibowo. Oxidative stress: Molecular mechanisms, role in pathology, and therapeutic implications. *Trends in Sciences* 2025; **22(12)**, 11462.

[61] S Anwar, T Sarwar, AA Khan and AH Rahmani. Therapeutic applications and mechanisms of Superoxide Dismutase (SOD) in different pathogenesis. *Biomolecules* 2025; **15(8)**, 1130.

[62] R Liu, J Yang, Y Li, J Xie and J Wang. Heme oxygenase-1: The roles of both good and evil in neurodegenerative diseases. *Journal of Neurochemistry* 2023; **167(3)**, 347-361.

[63] D Siegel, DL Gustafson, DL Dehn, JY Han, P Boonchoong, LJ Berliner and D Ross. NAD(P)H: Quinone oxidoreductase 1: Role as a superoxide scavenger. *Molecular Pharmacology* 2004; **65(5)**, 1238-1247.

[64] WS Lee, W Ham and J Kim. Roles of NAD(P)H: Quinone oxidoreductase 1 in diverse diseases. *Life* 2021;**11(12)**, 1301.

[65] SM Shin, JH Yang and SH Ki. Role of the Nrf2-ARE pathway in liver diseases. *Oxidative Medicine and Cellular Longevity* 2013; **2013**, 763257.

[66] JS Park, N Rustamov and YS Roh. The roles of NRF2-regulated oxidative stress and mitochondrial quality control in chronic liver diseases. *Antioxidants* 2023; **12(11)**, 1928.